Influence of Surface Roughness on the Pull-Off Force in Atomic Force Microscopy

Joonkyung Jang,*,† Jaeyoung Sung,‡ and George C. Schatz*,§

Department of Nanomaterials Engineering and BK21 Nanofusion Technology Team, Pusan National University, Miryang 627-706, Republic of Korea, Department of Chemistry, Chung Ang University, Seoul 156-756, Republic of Korea, and Department of Chemistry, Northwestern University, 2145 Sheridan Road, Evanston, Illinois 60208-3113

Received: October 10, 2006; In Final Form: January 14, 2007

We investigate how the pull-off force in atomic force microscopy (AFM), which arises from a nanoscale water bridge between the AFM tip and the surface, is influenced by atomic scale (smaller than 0.6 nm) roughness in the surface. Adopting a lattice gas model for water, we have simulated the adhesion of a silicon-nitride tip (with a 20nm diameter) to mica under ambient humidity. The pull-off force responds sensitively to both surface and tip roughness, and its humidity dependence changes significantly with slight variation in the tip and surface morphology. The change in the pull-off force due to roughness smaller than 0.6 nm can be larger than the change from doubling the tip radius. The roughness effect is large at low humidities and diminishes as humidity increases. Even at 80 percent humidity, the pull-off force varies considerably with changes in tip-surface geometry. On average, the pull-off force decreases with increasing tip roughness. However it decreases with surface roughness for small roughness (<0.2 nm), and then it increases for larger roughness. The pull-off force is also found to decrease with increasing average tip-surface distance at the point of initial contact, which shows the importance of spatial confinement of the water droplet.

1. Introduction

Under ambient humidity, a water bridge forms between an AFM tip and a surface. This nanoscale bridge exerts a substantial force on the AFM tip,[1−6] and the force needed to pull the tip away from the surface is known as the pull-off force. Understanding the factors which determine this force provides useful information for understanding the humidity-induced adhesion between two solid objects (e.g., powders and granular materials). This force also plays an important role in the molecular transport from the tip to the surface in dip-pen nanolithography.[7]

The macroscopic Laplace−Kelvin equation[2,6,8,9] has been widely used to study the water bridge and the resulting pull-off force. This continuum theory in its simplest form prescribes that the pull-off force is given as $4\pi R\gamma \cos\theta$, where R is the tip radius, θ the water-surface contact angle, and γ the surface tension of water. Accordingly, the pull-off force should show little humidity dependence. Various AFM experiments however have reported that the pull-off force is sensitive to humidity change.[2−6] This discrepancy is not surprising because many measurements involve conditions where the discrete size of the water molecules is important, and continuum approximations are not appropriate. The continuum theory incorrectly assumes that the water bridge shape can be described by two principal radii, and its volume remains unchanged as the tip is retracted. Any continuum theory also presumes that the periphery of the water bridge is fixed so that the bridge is stable to thermal fluctuation. This nanobridge however is often unstable (its periphery fluctuates) when the tip diameter is small (such as for a carbon nanotube) and the bridge is only a few molecules wide.[10] One can elaborate on the continuum theory by taking into account the existence of a surface water film and the nonspherical shape of the tip.[2] In spite of this effort, Xiao and Qian[2] have found that the continuum theory is not able to reproduce the experimental behavior of the pull-off force with respect to humidity. In addition to its quantitative failure in predicting the pull-off force, continuum theory has inherent difficulty in delivering molecular insights on the problem.

In past work,[11−14] we have studied the pull-off force by using grand canonical Monte Carlo calculations based on a lattice gas model. The same lattice model is able to capture the essential features of nanoscale confined water for a system that is similar to ours.[15] It also successfully explained experimental results concerning the self-assembly of nanoparticles.[16−18] We have used this model to simulate nanoscale water bridges like the one shown in Figure 1, and we have developed a thermodynamic integration method[12,13] to calculate the pull-off force from molecular Monte Carlo simulations. Our simulations reproduce the typical magnitude of the experimental pull-off force and its humidity dependence. This humidity dependence varies significantly as the tip wettability changes from hydrophobic to hydrophilic.[12]

In most of our past work, the theoretical interpretation of the pull-off force has relied on the notion that the tip and surface are smooth. At the atomic scale however, real materials inevitably are rough to some extent. One of our previous Monte Carlo study[11] has shown that small scale (less than 0.2 nm) roughness in the tip can lead to drastic differences in the pull-off force. The humidity dependence of the pull-off force could be understood by examining closely the structure of the water bridge that gives rise to the force. At low humidities, the water bridge is small so that it responds sensitively to the atomic-scale details of tip morphology. In this case the pull-off force mainly arises from a water bridge formed at a single or a small

* Corresponding authors. Email: jkjang@pusan.ac.kr, schatz@chem.northwestern.edu.
† Pusan National University.
‡ Chung Ang University.
§ Northwestern University.

10.1021/jp066667a CCC: $37.00
Published on Web 03/03/2007

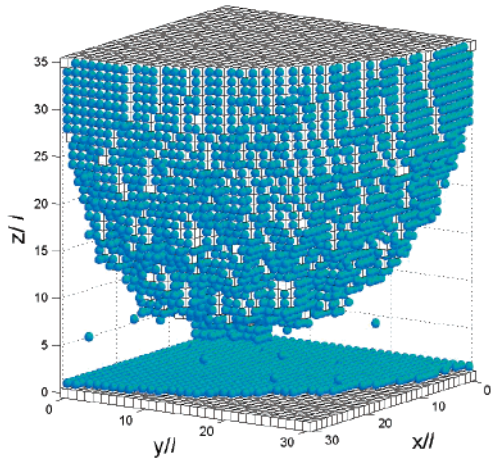

Figure 1. Computer-generated snapshot of the water bridge condensed between a hemispherical AFM tip and a flat surface. Lengths in the figure are in the units of the lattice spacing, l (0.37 nm), and the tip radius is 30 lattice spacings (11 nm). Water molecules are drawn as spheres. Tip and surface sites are represented as cubes. The relative humidity is set to 40%. Only the first quadrant ($x \geq 0$, $y \geq 0$) of our system is shown.

number of atomic-scale asperities on the tip. Therefore, the pull-off force changes significantly from tip to tip. As humidity rises, the bridge covers up many asperities, and the roughness effect of the tip on the pull-off force diminishes. If the tip is macroscopic in size, the pull-off force will be determined by the overall tip curvature only. Nanoscale (diameter of 20 nm) tips, however, are under the influence of atomic-scale roughness even at 80% relative humidity.

Our previous study focused on the roughness of the tip for a smooth surface. Herein, we investigate the effect of roughness in the surface as well. The surface differs from the tip in its large (infinite) radius of curvature, and we find that this leads to different effects on the pull-off force. It is also interesting to check whether there is a qualitative difference from the previous work if roughness exists for the both of interacting bodies, namely, the tip and surface as this case should be more relevant to real experiments. For an extensive set of tip and surface geometries (total of 49 tip−surface geometries), we investigate how the roughness in the surface affects the pull-off force. Also, by considering roughness larger than studied previously, we investigate how increasing roughness affects the pull-off force. We take into account a wide range of humidity (0−80%), and draw conclusions on how the pull-off force varies with various geometrical factors such as the degree of roughness and the spatial confinement of the system.

2. Simulation Details

We consider a system that consists of a hemispherical AFM tip above a planar surface (Figure 1). Water molecules can occupy cubic lattice sites confined between the tip and surface. Lengths are in units of the lattice spacing, l, which is taken to be the molecular diameter of water, 0.37 nm.[15] The radius of the tip R is taken to be 30 lattice spacings (11 nm), and the horizontal range of our system is $-30 \leq x, y \leq 30$. The first quadrant ($x \geq 0$, $y \geq 0$) of the system is simulated using a Monte Carlo method, and the remaining quadrants are taken to be mirror images of the first with respect to the XZ and YZ planes and the Z axis. Invoking this reflecting boundary condition yields nearly identical results to simulations that include the complete system.[12,13]

In the lattice model, each water molecule interacts with nearest neighbor molecules with an attraction ϵ and has its own chemical potential μ. When it is the nearest neighbor of one of the sites of the tip boundary and the surface, it feels the binding energies, b_T and b_S, respectively. (Herein, we use the term "tip boundary" instead of "tip surface" to prevent the readers from confusing it with the term "surface") The system Hamiltonian is

$$H = -\epsilon \sum_{i,j=\mathrm{nn}} c_i c_j - b_T \sum_{i=\mathrm{tip\ bound.}} c_i - b_S \sum_{i=\mathrm{surf.}} c_i - \mu N \quad (1)$$

where c_i is the occupancy (1 or 0) of the ith site, and the first summation runs over nearest-neighbor pairs, the second is for the sites next to the tip boundary, and the third for the sites right next to the surface. N is the number of molecules in the system. It is well known that the lattice model with a nearest neighbor interaction can reproduce collective phenomena such as gas−liquid condensation. The same nearest-neighbor lattice model has fully reproduced the main results of the atomistic simulation of the phase transition of water in a carbon nanotube.[15] Using the Hamiltonian, eq 1, we performed grand canonical (μVT) Monte Carlo simulations.[10−14] For given values of μ, V, and T, we have performed 40,000 Monte Carlo moves (trials to change c_i) for every site. The relative humidity, s, is defined as $s = \exp[(\mu - \mu_c)/k_B T]$, where μ is chemical potential and μ_c (-3ϵ) is the chemical potential at the bulk gas−liquid transition.[19] This definition is the ideal gas limit expression for the system pressure relative to the bulk saturation pressure. The bulk critical temperature T_c for the lattice gas is given by $k_B T_c/\epsilon = 1.128$. Identifying our liquid as water ($T_c = 647.3$ K) sets $\epsilon = 4.771$ kJ mol^{-1}. The temperature is fixed at $T/T_c = 0.46$, corresponding to water at room temperature (300K). If we use the above physical values for ϵ and l, our force unit is $\epsilon/l = 0.021$ nN. As before, energetic parameters are chosen to mimic a silicon-nitride tip interacting with mica: $b_T/\epsilon = 2.68$ and $b_S/\epsilon = 2.47$.[11] In calculating the bulk density ρ, we use mean-field density functional theory (DFT).[20] With this approach, the grand potential per unit volume Ω_{DFT}/V is given by

$$\Omega_{DFT}/V = k_B T[\rho \log \rho - (1-\rho)\log(1-\rho)] - 3\epsilon\rho^2 - \mu\rho \quad (2)$$

The equilibrium density is determined by the condition, $\delta\Omega_{DFT}/\delta\rho = 0$. We checked the validity of DFT by running several simulations for the bulk system, and quantitative agreement with Monte Carlo simulations was found.

The adhesion force F between the tip and surface separated by a distance h is given by[21]

$$\left(\frac{\partial F}{\partial \mu}\right)_{h,T} = \left(\frac{\partial N_{ex}}{\partial h}\right)_{\mu,T} \quad (3)$$

where N_{ex} is the excess number of molecules with respect to bulk ($N_{ex} = N - N_{bulk}$). We first calculate F versus h by numerically integrating eq 3 with respect to μ (thermodynamic integration).[12,13] At a fixed temperature T and chemical potential μ, F is a function of h. A typical F is negative (attractive) for small h and approaches zero as h increases. Occasionally, F is repulsive ($F(h) > 0$) when the tip is in direct contact with the surface, i.e., $h = l$. This is the case where the contact of the tip with the surface squeezes many molecules out of the confined space between the tip end and the surface.[11] We identify the magnitude of the minimal $F(h)$ as the pull-off force. In most cases of our simulation (total of 4754 cases), $F(h)$ has its minimum value at $h = l$ (66% of the cases) or $h = 2l$ (33% of

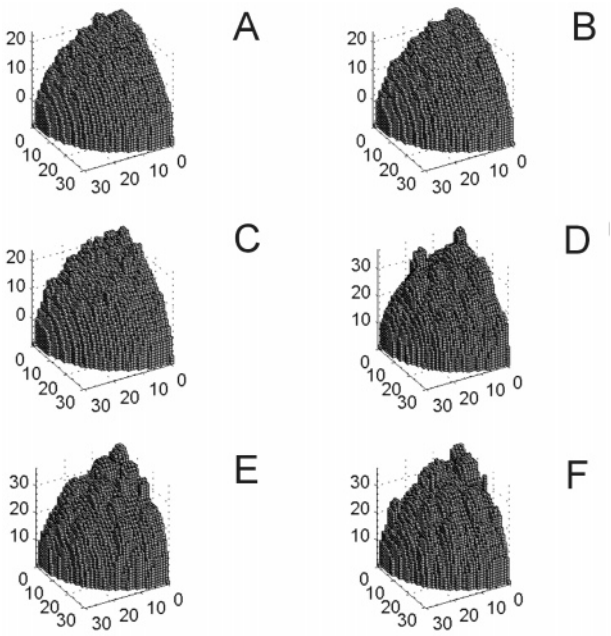

Figure 2. Pictures of the six rough tips that were simulated. Tip sites are represented as cubes. Lengths in the figure are in units of the lattice spacing (0.37 nm) and the tip radius is 30 lattice spacings (11 nm). Only the first quadrant of each tip is shown. Each tip is drawn upside down for visual clarity. The rms roughness for tips A, B, C, D, E, and F is 0.20, 0.19, 0.22, 0.60, 0.59, and 0.57 nm, respectively.

the cases). For the rest 1% of the cases, the force becomes minimal at a longer distance ($h = 3l$, $4l$, and $5l$). This long ranged force minimum occurs at a high humidity near 80%. For this humidity, the corresponding water bridge is large in size and the tip−surface force becomes long-ranged (which has been observed in reference 13). This shows that our nearest neighbor interaction without direct tip−surface interaction does produce a long-ranged force. The short-ranged force minimum found in most cases arises from the small size of the underlying water bridge, which is in turn due to low humidity and the sharp asperity of the nanoscale tip. If humidity becomes higher than 80% and the tip has a larger radius, we will observe a long-ranged force as we have seen in 1% of the cases.

We simulated seven different AFM tips to study tip roughness effects. One of them is a smooth hemispherical tip defined as the collection of lattice sites closest to a continuous hemispherical surface with a radius of 30 lattice spacings. We also considered the six rough tips drawn in Figure 2. A rough tip is generated by changing the Z coordinates of the smooth tip boundary as follows. Starting with the smooth tip, we choose an arbitrary point on the tip boundary, and introduce a small hemispherical bump with a randomly selected radius that is taken from a Gaussian distribution with a variance of 0.74 nm (for tips A−C) or 1.44 nm (for tips D−F). Then the Z positions of the smooth tip boundary are changed by adding the hemispherical bump to the tip boundary. This addition process is repeated until there is no tip boundary area available for additional bumps. Each hemispherical bump is not allowed to overlap any of the bumps already produced. Tips A, B, and C have root-mean-square (rms) roughness of 0.20, 0.19, and 0.22 nm, respectively (where the roughness is defined as the rms deviation of the Z positions of the rough tip from those of the smooth tip). These roughness values are similar to those considered previously.[11] Tips D, E, and F have rms roughnesses of 0.60, 0.59, and 0.57 nm, respectively, nearly 3 times larger than those of tips A, B, and C.

We examined seven different surfaces, one of which is a flat square lattice located at $Z = 0$. The 6 rough surfaces drawn in Figure 3 are generated by introducing hemispherical bumps with random radii and locations to the flat square lattice. As in generating the rough tips above, we have sampled the radius of the hemispherical bump from a Gaussian distribution with a variance of 0.74 nm (for surfaces a−c) or 1.44 nm (for surfaces d−f). Then hemispherical bumps are added to the flat surface. And this addition is repeated until there is no surface area available for additional bumps (as in the tip, each bump is not allowed to overlap any of the bumps already produced). Surfaces a, b, and c have rms roughnesses of 0.24, 0.22, and 0.22 nm, respectively, where surface roughness is defined as the rms deviation of the Z positions of the rough surface from those of the smooth surface. Surfaces d, e, and f have rms roughnesses of 0.59, 0.54, and 0.60 nm, respectively, and are thus about three times bigger in roughness than surfaces a−c.

3. Results and Discussions

Let us first examine how tip size affects the pull-off force. In Figure 4, the pull-off force for a smooth tip on a smooth surface is plotted as a function of RH. As we increase the tip radius r from 11.1 to 14.8 and 18.5 nm, the pull-off force for a given humidity increases. This seems reasonable because, for a larger tip, a bigger water bridge forms between the tip and surface. A bigger bridge should yield stronger adhesion between the tip and surface. Notice however that the humidity dependence of the pull-off force does not change with tip size.

Figure 5 shows how the pull-off force responds if we change the morphology of the tip, instead of the tip size. The pull-off force varies radically by roughening the tip, especially at low humidities. The difference in the force can be larger than 6 nNs at close to 6% RH. This is remarkable because making the tip radius 1.7 times larger (from 11.1 to 18.5 nm) yielded at most a 5nN difference in the pull-off force (Figure 4) but a roughness of less than 0.6 nm makes a 6 nN difference. In addition, the humidity dependence of the pull-off force changes drastically with tip roughness. Notice that tips A−C have the similar roughness and are not much different in shape from each other. Likewise, tips D−F are similar to each other. The pull-off force of the smooth tip initially increases and then decreases as RH increases. The pull-off force for the rough tips is more varied in its humidity dependence. For some of the rough tips, the pull-off force initially increases, then decreases, and then increases again as we raise RH. Some rough tips show a nearly monotonic increase in pull-off force as RH rises. As RH approaches 80%, the pull-off force of each tip becomes similar, but not exactly the same. This means that even at this high humidity, the underlying water bridge can sense the roughness of the nanometer AFM tip.

On the whole, the pull-off force of the smooth tip is larger than that of a rough tip. And the tips with small roughness (tips A−C in Figure 2, drawn as open symbols) have larger pull-off forces than the tips with large roughness (tips D−F in Figure 2, drawn as filled symbols). The reason behind this trend can be related to the fact that the smooth tip has the largest tip−surface contact area (defined as the area of the tip which touch the surface at the closest approach of the tip to the surface, $h = l$[10,11]). As we mentioned previously,[11] the pull-off force is mainly governed by (especially at low RHs) the number of molecules which face both the tip boundary and the surface. The number of such molecules is proportional to the tip−surface contact area, and the smooth tip has the largest contact area among all the tips.

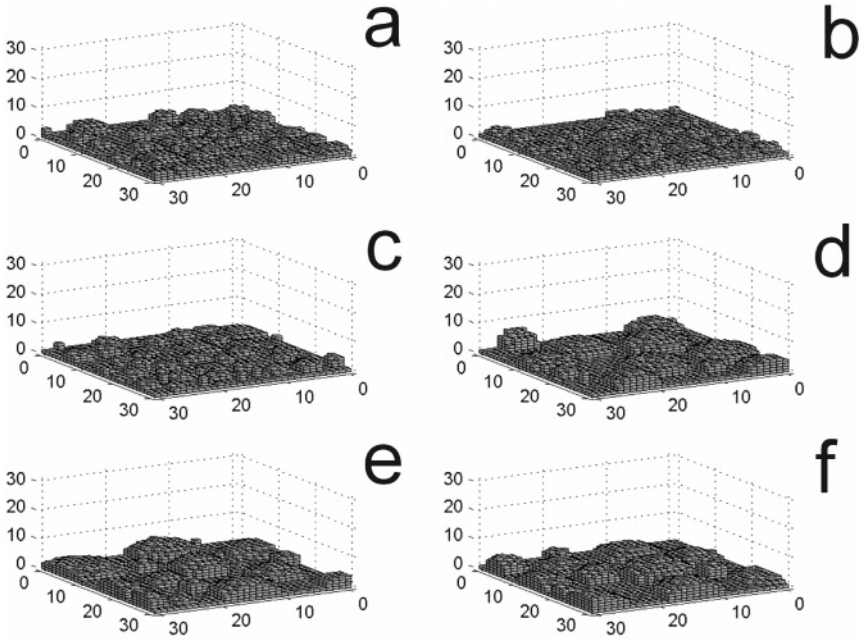

Figure 3. Pictures of the six rough surfaces that were simulated. Surface sites are represented as cubes. As in Figure 2, only the first quadrant is shown (the rest is a mirror image of the figure). The rms roughness for surfaces a, b, c, d, e, and f is 0.24, 0.22, 0.22, 0.59, 0.54, and 0.60 nm, respectively.

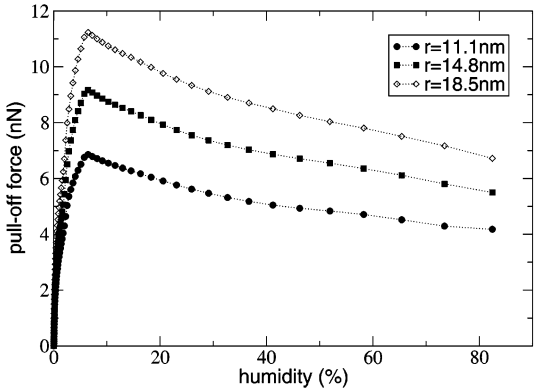

Figure 4. Tip size effect on the pull-off force. The pull-off force vs humidity is drawn for a smooth tip on a flat surface. We have drawn the pull-off force for tips with radii of 11.1, 14.8, and 18.5 nm. In this and all the following figures, lines are drawn to guide the eyes.

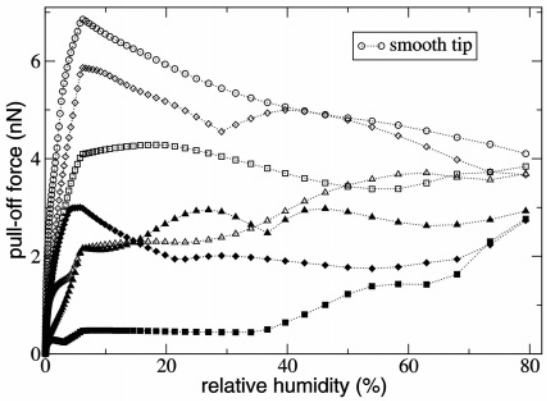

Figure 5. Effect of tip roughness on the pull-off force. For the smooth surface, the pull-off force vs humidity is drawn for the smooth tip (drawn as circles) and the rough tips of Figure 2. Open symbols represent tips A−C in Figure 2. Filled symbols correspond to tips D−F in Figure 2.

We now investigate how the roughness of the surface affects the pull-off force. In Figure 6, we plot the humidity dependent pull-off force for a smooth tip on various surfaces. One can see that this roughness also profoundly changes the pull-off force. The roughness effect is especially significant at low humidities (<20%). The pull-off force of a rough surface can be nearly 5 nN smaller than that of the smooth surface. The difference in the force gets small as RH approaches 80%. As with the tip roughness, this is ascribed to the fact that the underlying water bridge is narrow at a low humidity and is very sensitive to little bumps on the surface. At high humidities, the bridge becomes wide and covers up the small bumps, so that the atomic details of the surface do not play an important role. Even at the highest humidity however, we see a difference in the pull-off force for different surfaces. Again, this means that the size of the underlying water bridge did not reach the macroscopic limit, and therefore the resulting pull-off force reflects the atomic-scale morphology of the surface to some extent. Notice that the pull-off force of a rough surface can be greater than that of the smooth surface especially at high RHs. Although it has a tip−surface contact area smaller than the smooth surface, a rough surface has gorges between the bumps on the surface. When the water bridge fills in these gorges, molecules feel a stronger binding from the surface than from a smooth surface (because molecules in these gorges are more confined by the surface walls). The stronger molecular binding to the surface gives rise to a stronger pull-off force. This extra strength sometimes can overcome the decrease in the pull-off force due to a smaller tip−surface contact area for the rough surface.

Let us investigate the case of a rough tip on a rough surface (which should be a better model of real experiments). In Figure 7, we plot the pull-off force versus RH for tip D in Figure 2 on various surfaces. Again, the pull-off force and its humidity dependence change drastically by switching the tip−surface combination. Here, we see a weaker convergence of the pull-off force at high RHs compared to the case where either the tip or the surface is smooth. Even at 80% RH, the difference in the pull-off force can be as large as about 3 nNs. Since both the tip and the surface are rough, the systems in Figure 7 are

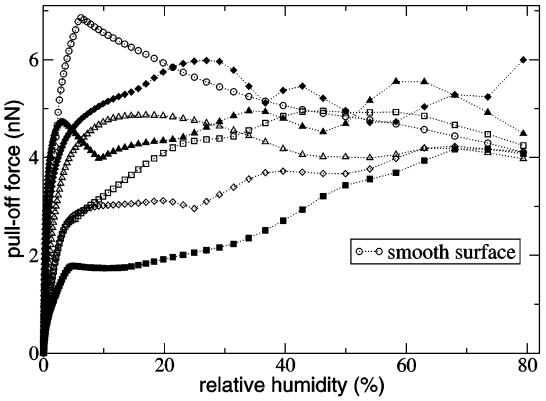

Figure 6. Effect of surface roughness on the pull-off force of the smooth tip. We plot the pull-off force vs humidity for the smooth surface (drawn as circles) and for six rough surfaces shown in Figure 3. Open symbols represent surfaces a−c of Figure 3. Filled symbols correspond to surfaces d−f in Figure 3.

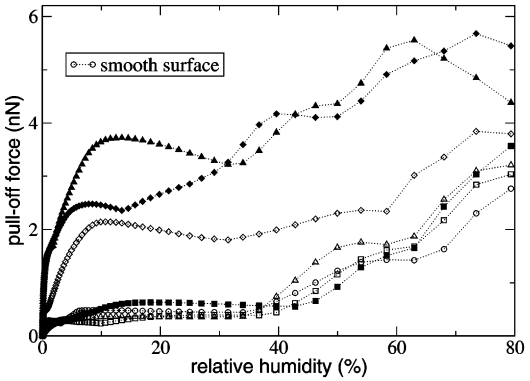

Figure 7. Pull-off force for a rough tip on a rough surface. For tip D in Figure 2, we plot the pull-off force vs humidity for the smooth surface (drawn as circles) and for the six rough surfaces shown in Figure 3. Open symbols (filled symbols) correspond to surfaces a−c (surfaces d−f).

more corrugated than those for which roughness exists only in the tip (Figure 5) or in the surface (Figure 6). A more corrugated system is more sensitive to the tip and surface geometry, and this sensitivity turns out to persist up to RH of 80%. Here, some of the rough surfaces have the pull-off force much larger than that of the smooth surface for the entire range of RH. This is due to the fact that some surfaces geometrically match the particular tip of Figure 7 (tip D) more than the smooth surface does. That is, for two of the rough surfaces, the tip shape matches the surface morphology so that the free volume between the tip and surface is small compared to other surfaces. In this case, the system is more confined between the tip and surface, and an increased confinement leads to an increased pull-off force. Later, we will examine this point further.

Figure 8 shows the pull-off force averaged over all the possible tip−surface geometries (total of 49 cases). The geometry-averaged force for a given RH is plotted along with its standard deviation (drawn as an error bar). This geometry averaged pull-off force monotonically increases with humidity. The force shows a steep increase at low RHs followed by a gradual ascent at high RHs. One can see that the fluctuation in force due to geometry change is quite large at low RHs. The standard deviation in the pull-off force can be as large as 88% of its average. As RH increases, the standard deviation of the force decreases but it is significant (about 2 nN, 21% of its average) even at a RH of 80%.

We have seen in Figure 5 that the pull-off force of a rough tip on a smooth surface is smaller than that of the smooth tip.

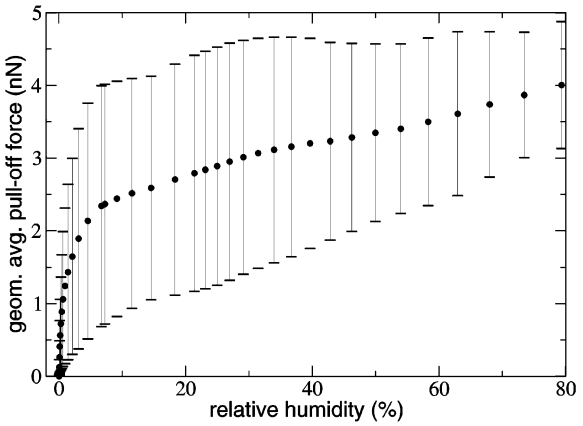

Figure 8. The pull-off force averaged over various tip and surface geometries. We calculated the pull-off force for all the possible combinations of the tip and surface and then averaged. Error bars show the rms deviations.

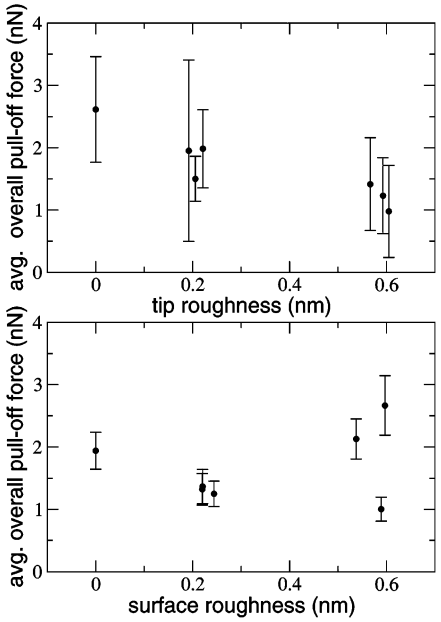

Figure 9. The average overall pull-off force vs the degree of roughness. [Top] For each tip, the overall pull-off force is averaged over seven different surfaces. This average overall pull-off force is plotted vs the corresponding tip roughness. Error bars represent the rms deviation in the force. [Bottom] For each surface, the overall pull-off force is averaged over seven different tips. This average pull-off force is shown as a function of the surface roughness. Error bars show the rms deviations.

Also, as seen in Figures 6 and 7, a rough surface sometimes gives rise to a pull-off force larger than that of a smooth surface. We have checked whether roughness in the tip reduces the pull-off force regardless of the surface geometry as well as whether roughness in the surface on the whole increases or decreases the pull-off force. To do so, we have first averaged the pull-off force for a given tip−surface geometry over RH (0−80%). We call this average the overall pull-off force for a given tip−surface geometry. Since the dependence of this overall pull-off force on tip roughness varies from surface to surface, we have averaged, for a given tip, the overall pull-off force over the seven different surfaces of our simulation. The top of Figure 9 illustrates how this geometry-averaged overall pull-off force varies with tip roughness. The error bars are the standard deviations in the average over the surface geometry. Note the large error bars and that the difference due to the tip roughness is less than 1.7 nNs. Nevertheless, the figure shows that this

average overall pull-off force decreases with increasing tip roughness. To confirm this trend, we have statistically tested the correlation between the tip roughness and the overall pull-off force. For all the tip−surface combinations (49 cases), we have calculated the linear correlation coefficient r (Pearson's r) between the tip roughness and overall pull-off force.[22] We found that r is −0.47 (negative correlation) with the significance level (at which the tip roughness and the overall force are uncorrelated) being 0.058%. This strongly supports our claim that the overall pull-off force decreases with increasing the tip roughness.

An analysis similar to that done in the top of Figure 9 can be applied to surface roughness. The resulting pull-off force versus surface roughness is presented in the bottom of Figure 9. Here, the pull-off force for a given surface is averaged over the seven different tip geometries. Error bars represent standard deviations in the geometry average over tips. Here, the error bars are smaller than those in the top of Figure 9, meaning that the variation in pull-off force due to tip change is smaller than that due to the change in the surface morphology. Increasing the surface roughness from zero to about 0.2 nm makes the average overall pull-off force smaller. Further increasing the roughness to around 0.6 nm increases the average overall pull-off force for two of the three roughest surfaces. In contrast, the average pull-off force for the remaining surface is smaller compared to that for surfaces with 0.2 nm roughness. This split behavior might arise from the limited number of tip geometries sampled in our simulation. On average however, we can say that for 0.6 nm surface roughness the overall pull-off force increases. To corroborate this, we have performed a statistical test for the correlation between the tip roughness and the overall pull-off force. First, we have chosen the tip−surface combinations with surface roughness less than 0.3 nm (there are 28 such combinations). The linear correlation coefficient between the surface roughness and the overall pull-off force, r, is −0.36 with a significance level of 6.0%. This tells us that the overall pull-off force indeed decreases with increasing the substrate roughness from zero to 0.22 nm. Next, we have considered surface roughnesses of 0.22 nm and higher (there are 28 tip−surface combinations corresponding to this case). The statistical correlation coefficient between the surface roughness and the overall pull-off force r is found to be 0.64 with a significance level of 0.027%. This statistically maintains that the overall pull-off force increases with increasing surface roughness from 0.22 up to 0.60 nm.

The pull-off force originates from water condensation, which is in turn due to confinement between the tip and surface. It is then reasonable to expect that increased confinement will lead to a bigger water bridge and an enhanced pull-off force. To quantify what we mean by confinement, we have chosen the average vertical distance between the tip and surface. This average distance is defined as follows. For a tip−surface distance corresponding to direct contact ($h = 0.37$ nm), we calculate, for each lattice site of the tip boundary, the distance from the tip boundary site to the surface site right below. The average distance between tip and surface is then given by the average of this vertical distance. The lateral extent of the tip is a circular disk with 11 nm radius (the tip radius), so this average vertical distance is representative of the free volume of water between the part of the tip and surface where there is direct contact. The larger the average distance, the less confined is the system. In Figure 10, the average tip−surface distance is plotted against the overall pull-off force. Error bars represent the rms deviation of the overall pull-off force with respect to RH. The figure shows that, on average, the overall pull-off force decreases as the average tip−surface distance increases. A statistical test for the correlation between the average distance and the pull-off force shows the linear correlation coefficient r and the significance level are −0.81 and 1.3×10^{-10}%, respectively. Therefore, there is a strong negative correlation between the tip−surface distance and the pull-off force. There is, however, a small exception to this trend at an average distance of 4.4 nm, where the overall pull-off force is bigger than at 4 nm. This arises from the presence of gorges in the rough surface (in this case, surface f in Figure 3). As described earlier, molecules confined in these gorges are more strongly attracted to the surface than molecules on a flat surface. These molecules can give extra strength to the pull-off force that can overwhelm the decrease in the vertical confinement. The average vertical distance does not incorporate the presence of these gorges and the enhanced confinement due to them, but this effect is small.

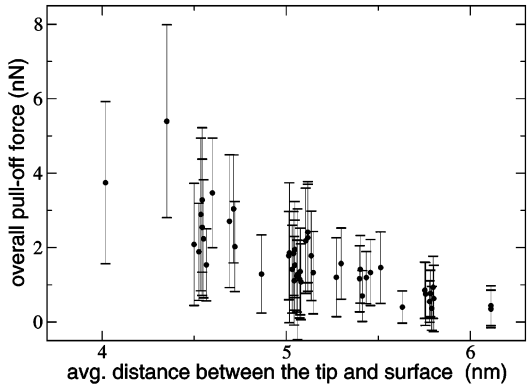

Figure 10. Correlation between the overall pull-off force and the degree of confinement. The overall pull-off force is plotted vs the average vertical distance between the tip and surface. Error bars represent the rms deviation (with respect to RH) of the overall pull-off force.

The current simulation has been based on a short-ranged (nearest neighbor type) molecular interaction. Inclusion of the long-range molecular interaction might yield water bridges bigger in size than obtained here. This might reduce the roughness effects because a bigger bridge can cover up the small bumps on the tip and surface. Note however that we have continuously changed humidity from 0 to 80% and taken into account various sizes (from small to large relative to the roughness scale) of water bridge. And we have seen that our short-ranged interaction does produce a long-ranged pull-off force. The present work is mainly concerned about how the pull-off force varies as we change humidity (therefore, the size of the water bridge). If we include the long-ranged molecular interaction in our simulation, there might be some quantitative difference, for example, in the exact value of humidity at which the pull-off force changes its humidity dependence (from increasing to decreasing). The qualitative behavior of pull-off force regarding humidity will remain intact however.

Since the surface roughness changes the pull-off force significantly, one can deduce that the pull-off force on a rough surface should vary if the tip changes its lateral position. It would be interesting to compute this position dependent pull-off force and compare it with experiment if possible.

4. Conclusions

The present Monte Carlo simulation of the pull-off force in AFM reveals that roughness of the surface as well as of the tip fundamentally changes the pull-off force measurement. Intro-

ducing roughness less than 0.6 nm to the tip or surface can change the pull-off force by more than arises from doubling of the tip radius. At low humidities in particular, even a slight roughening in the tip or surface leads to a drastic difference in the pull-off force. As humidity approaches 80%, the roughness effect diminishes but never goes away for our 20 nm wide AFM tips. The pull-off force at a low humidity originates from a water bridge condensed between small asperities. The resulting pull-off force reacts sensitively to the atomic details of the tip and surface geometries. As the tip−surface geometry changes, the fluctuation in the pull-off force can be as large as 82% of its average value. As humidity is increased, the water bridge covers up small asperities, and details of the tip and surface morphology play a less important role. In contrast to what would be expected for a macroscopic system, the roughness effect persists even at 80% humidity for our nanoscale system, where the variation in pull-off force due to roughness amounts to 20% of its average value. After examining 49 tip−surface geometries, we conclude that on-average roughness in the tip decreases the pull-off force. In contrast, although small roughness in the surface decreases the pull-off force, further increases lead to an increase. Overall, the pull-off force increases as the free volume between the tip and surface decreases (as the system gets more confined).

Acknowledgment. This work was supported by the Korea Research Foundation Grant funded by the Korean Government (MOEHRD, Basic Research Promotion Fund) (Grant No. 2005-070-C00065). JJ thanks Prof. Cho Young Seuk for his help on statistical tests. GCS was supported by a grant from the National Science Foundation (grants CHE-0550497 and EEC-0647560).

References and Notes

(1) Choe, H.; Hong, M.-H.; Seo, Y.; Lee, K.; Kim, G.; Cho, Y.; Ihm, J.; Jhe, W. *Phys. Rev. Lett.* **2005**, *95*, 187801.
(2) Xiao, X.; Qian, L. *Langmuir* **2000**, *16*, 8153.
(3) Sedin, D. L.; Rowlen, K. L. *Anal. Chem.* **2000**, *72*, 2183.
(4) Asay, D. B.; Kim, S. H. *J. Chem. Phys.* **2006**, *124*, 174712.
(5) He, M.; Blum, A. S.; Aston, D. E.; Buenviaje, C.; Overney, R. M.; Luginbuhl, R. *J. Chem. Phys.* **2001**, *114*, 1355.
(6) Butt, H-J; Farshchi-Tabrizi; Kappl, M. *J. Appl. Phys.* **2006**, *100*, 024312.
(7) Ginger, D. S.; Zhang, H.; Mirkin, C. A. *Angew. Chem., Int. Ed.* **2004**, *43*, 30.
(8) Fisher, L. R.; Israelachvili, J. N. *J. Colloid Interface Sci.* **1981**, *80*, 528.
(9) Gao, C. *Appl. Phys. Lett.* **1997**, *71*, 1801.
(10) Jang, J; Schatz, G. C.; Ratner, M. A. *Phys. Rev. Lett.* **2004**, *92*, 85504.
(11) Jang, J.; Ratner, M. A.; Schatz, G. C. *J. Phys. Chem. B* **2006**, *110*, 659.
(12) Jang, J.; Schatz, G. C.; Ratner, M. A. *J. Chem. Phys.* **2004**, *120*, 1157.
(13) Jang, J.; Schatz, G. C.; Ratner, M. A. *Phys. Rev. Lett.* **2003**, *90*, 156104.
(14) Jang, J.; Schatz, G. C.; Ratner, M. A. *J. Chem. Phys.* **2002**, *116*, 3875.
(15) Maibaum, L.; Chandler, D. A. *J. Phys. Chem. B* **2003**, *107*, 1189.
(16) Yosef, G.; Rabani, E. *J. Phys. Chem. B* **2006**, *110*, 20965. Sztrum, C. G.; Hod, O.; Rabani, E. *J. Phys. Chem. B* **2005**, *109*, 6741.
(17) Sztrum, C. G.; Rabani, E. *Adv. Mater.* **2006**, *18*, 565.
(18) Rabani, E.; Reichman, D. R.; Geissler, P. L.; Brus, L. E. *Nature* **2003**, *426*, 271.
(19) Pandit, R; Schick, M.; Wortis, M. *Phys. Rev. B* **1982**, *26*, 5112.
(20) De Oliveira, M. J.; Griffiths, R. B. *Surf. Sci.* **1978**, *71*, 687.
(21) Ash, S. G.; Everett, D. H.; Radke, C. *Faraday Trans. II* **1973**, *69*, 1256.
(22) Press, W. H.; Teukolsky, S. A.; Vettering, W. T.; Flannery, B. P. *Numerical Recipes in C*; Cambridge: New York, 1988.